Remote Monitoring and Control of the 2-DoF Robotic Manipulators over the Internet

Sadra Hokmi [a], Shahab Haghi [b], Alireza Farhadi [c],

[a] *BSc. student at the Department of Electrical Engineering, Sharif University of Technology, Tehran, Iran.*

[b] *BSc. student at the Department of Electrical Engineering, Sharif University of Technology, Tehran, Iran.*

[c] *Associate Professor at the Department of Electrical Engineering, Sharif University of Technology, Tehran, Iran.*

Abstract

This paper is concerned with remote monitoring and control of the 2-DoF robotic manipulators, which have nonlinear dynamics over the packet erasure channel, which is an abstract model for communication over the Internet, WiFi or Zigbee modules. This type of communication is subject to imperfections, such as random packet drop out and rate distortion. These imperfections cause a significant challenge for monitoring and control of robotic manipulators in the industrial environments because sensitive data, such as sensor data and control commands may not never reach to their destination resulting in significant performance degradation. Therefore, the effects of these imperfections must be compensated. In this paper we apply two coding and control techniques previously developed for the tele-presence ad tele-operation of autonomous vehicles to compensate the effects of the above communication imperfections for remote monitoring and control of the 2-DoF robotic manipulators controlled over the packet erasure channel. To achieve this goal, we design a new linear controller and a new nonlinear controller for the 2-DoF robotic manipulators over the packet erasure channel. The first technique is based on the linearization method and the second technique uses a nonlinear controller. The performances of these two techniques for remote monitoring and control of robotic manipulators are evaluated and compared with each other in this paper. We illustrate their satisfactory performances in the presence of severe communication imperfections.

Key words: Tele-presence; tele-operation; robotic manipulator; Industrial Internet of Things (IIoT), the Industry 4.0.

---

1 Introduction

In recent years, extensive research activity has been devoted to the tele-presence and tele-operation of robotic manipulators and autonomous vehicles (drone, autonomous road vehicle, autonomous underwater vehicle) due to its vast applications in the Industry 4.0, telesurgery, military, space and underwater exploration, smart agriculture,etc. [1] - [4]. In tele-robotic scenarios, a human operator or an intelligent control unit controls the movement of a robot from some distance away using very often wireless links. From the control theoretical point of view, the main goals of tele-robotic are two folds: Reference tracking (tele-operation) and tele-presence. Reference tracking means the tracking of a desired path designed by remote human operator/intelligent control unit; and tele-presence means providing the states of remotely controlled robot for human operator/intelligent control unit in real time so that remote human operator/intelligent control unit is able to design a proper desired path/control command for the satisfactory remote reference tracking. In tele-robotic applications, these two tasks are complicated since the communication medium contributes to the complexity of the problem by introducing delay, rate distortion, noise, fading, random packet drop out, etc. The focus on most of the tele-robotic papers has been on the communication delay, e.g., [2] - [11]. However, most of tele-robotic systems particularly those that are used in the industrial environments are subject to other types of communication imperfections, such as limited transmitter power constraint/bit rate constraint, noise, fading, random packet drop out and rate distortion. For example, in the problem of the tele-operation of a battery powered drone, which is becoming very popular due to its vast applications in transportation to remote locations, forestry, mining, agriculture, surveillance, search and rescue missions, etc., the tele-robotic system is subject to the limited power supply; and therefore, the transmission of information from drone to remote

---

Email address: `afarhadi@sharif.edu` (Alireza Farhadi).

human operator is subject to the minimum transmission power constraint; and hence, it is subject to noise and limited bit rate constraint. This results in random packet drop out and rate distortion imperfections meaning that some of the packets sent by drone to remote human operator are erased at the receiver side; because they contain unrecoverable filliped bits. Also, as each real valued measurement is represented by a small length packet (due to limited bit rate constraint), if the packet is recovered at the receiver, the real valued measurement will be recovered with some quantization error at the receiver. Nevertheless, the remote control station, where human operator is located, can be supplied with high transmission power in this tele-operated system; and hence, the transmission of information from remote human operator/intelligent control unit to drone can be assumed almost without communication imperfections. This can be represented by the block diagram of Fig. 1. Note that the compensation of the impacts of arbitrary transmission delay in the presence of random packet loss is on going research direction in the field of bilateral tele-operation systems. Some of the available papers addressing this problem in the context of tele-operated systems are [12] - [14]. [12] is concerned with linear dynamic systems over a communication network subject to arbitrary time delay. It considers the packet loss as the infinite time delay. [13] and [14] are also concerned with linear dynamic systems over a communication network subject to arbitrary time delay and the packet loss. The packet loss in these papers is modeled by the real erasure channel. That is, the delayed sensor measurement is either successfully received (without quantization error) or erased. However, the transmission of measurements over a communication link is subject to unavoidable rate distortion due to the quantization of real valued measurements to short length packets to be sent over a digital communication link. Hence, more suitable communication model for the transmission over a communication network is the packet erasure channel considered in this paper, which is described in Section 2. One of the early work on the tele-operation over the packet erasure channel is [15]. This paper is concerned with linear dynamic systems. [15] has motivates other works, such as [16] and [17], which are concerned with nonlinear dynamic systems over the packet erasure channel.

We have shown in our paper [16] that the aforementioned imperfections (the random packet drop out and the rate distortion) result in significant performance degradation. In [16] we presented a technique for remote monitoring and control of a quit general class of nonlinear dynamic systems in the presence of the random packet drop out and rate distortion without considering the impacts of actuators constraint. In the aforementioned paper, we used the linearization method to linearize the nonlinear dynamic system around the working points and then for the linearized systems we used one of the available techniques for linear networked control system. Other technique for remote monitoring and control of nonlinear dynamic systems subject to the random packet drop out can be found in [17]. In [17] we proposed a new technique, which directly involved nonlinear dynamics for the development of nonlinear tele-operated systems.

The new industrial movement known as the Industry 4.0 or smart manufacturing [18] is another major motivation for considering other types of communication imperfections and especially the random packet drop out and the rate distortion imperfection in tele-robotic problems. The new industrial movement has started around 10 years ago and is still a concept; but it soon becomes a reality. It aims to integrate production facilities, supply chains and service systems via the established information technology infrastructures, such as the Internet for the rapid decision making resulting in increasing productivity. In the Industry 4.0 - based manufacturing systems, each production facility, such as a robotic manipulator is equipped with at least one Industrial Internet of Things (IIoT) wireless communication module; and therefore, it can broadcast its sensor data to every corner of manufacturing factory and even outside manufacturing factory; while receiving high level commands from distributed decision makers. Due to the high level of noise in the industrial environments and because such environments are very often crowded environments, this real time remote monitoring and control is subject to severe random packet drop out and also limited bit rate constraint and hence rate distortion imperfection. Fig. 2 illustrates a typical IIoT system for manufacturing industry.

In this paper we focus on the problem of tele-presence and tele-operation of the 2-DoF robotic manipulators as shown by the block diagram of Fig. 1 over the packet erasure channel, which is an abstract model for the transmission via the Internet, WiFi and Zigbee modules. In this basic block diagram, the communication from sensor to remote controller is subject to the random packet drop out and rate distortion imperfection. However, there is no communication imperfection in the reverse direction. This is the case, for example, where the decision maker is co-located with robotic manipulator; while sensor (e.g., a camera watching the movement of the end-effector of the manipulator) is geographically separated from the manipulator (dynamic system) and transmits the collected sensor data to remote controller via a WiFi wireless link for example. In this basic block diagram there is a feedback acknowledgment from the receiver to transmitter. This feature is supported by the WiFi TCP/IP protocol and also many IIoT modules, such as Digi Xbee Pro. Note that in the aforementioned set up, long delayed packet is considered as the lost packet.

In this paper, we apply the coding and control techniques developed in [16] and [17] for remote monitoring and control of robotic manipulators over the Internet, which is modeled by the packet erasure channel. The coding and control techniques of [16] and [17] were

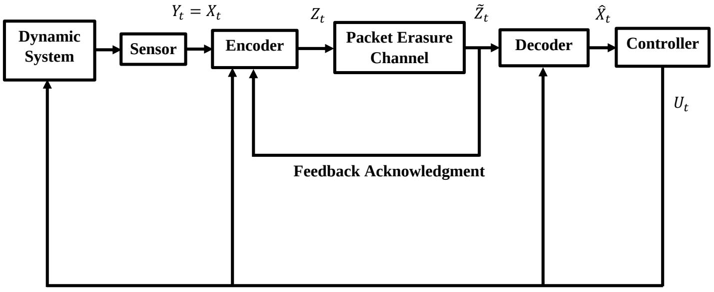

Fig. 1. A basic block diagram for remote monitoring and control over the Internet

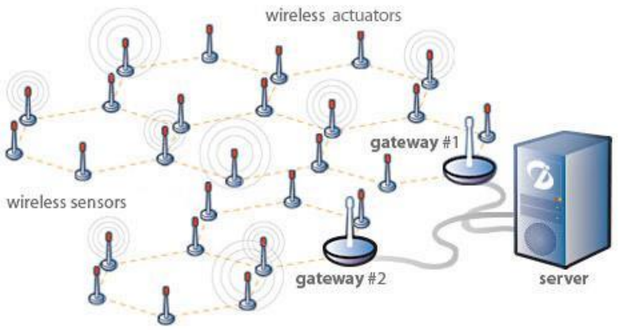

Fig. 2. A typical IIoT system for the Industry 4.0. This figure was borrowed from [19]

developed for the tele-presence and tele-operation of autonomous vehicles. However, in this paper we illustrate their applications for the tele-presence and tele-operation of robotic manipulators by designing proper linear and nonlinear controllers over the packet erasure channel. In the block diagram of Fig. 1, the encoder by the knowledge of the decoder law and the controller law and the feedback acknowledgment can determine the control command, U_t, applied on the manipulator. Under the aforementioned set up, we implement our techniques presented in [16] and [17] to design proper encoder, decoder and controller for the block diagram of Fig. 1 (described by a robotic manipulator) that result in a satisfactory tele-presence and tele-operation in the presence of severe random packet drop out and rate distortion imperfection. Using extensive computer simulations we illustrate the satisfactory performances of these techniques; and we compare their performances with each other for the remote monitoring and control of robotic manipulators. It is shown that both techniques result in a satisfactory performance provided the bound constraints for the applied torques on manipulator joints are satisfied.

As mentioned above, the focus on most of the tele-robotic papers has been on the communication delay, e.g., [2] - [11]; or the communication delay in the presence of the real erasure channel, e.g., [12] - [14]. However, most of the tele-robotic systems particularly those that are used in the industrial environments are subject to other types of communication imperfections, such as the random packet drop out and rate distortion imperfection; and this paper presents two suitable techniques for this type of tele-robotic systems. This is one of the major contributions of this paper. The first technique presented in this paper requires frequent linearization of nonlinear dynamic of manipulator and the data transmission with different bit rates at different linearization zones. It also requires a large bit rate when the erasure probability of the communication channel is large. Nevertheless, the other technique presented in this paper does not require the frequent model update and it involves a fixed and relatively small bit rate; but it requires more powerful processors because it is computationally expensive. Therefore, depending on the situation we have two different available techniques for remote monitoring and control of robotic manipulators over the Internet. When the bit rate constraint is sever the second technique is recommended. But, when there is sever computational constraint, the first technique is recommended. In summary, the major contributions of this paper are as follows:

- The presentation of a new linear controller and a new nonlinear controller for the tele-operation of the 2-DoF robotic manipulators over the Internet by considering the effects of unavoidable packet lost and rate distortion

- The illustration of the applicability of the coding techniques of [16] and [17] for the tele-presence of robotic manipulators

- The presentation of a new technique for remote monitoring and control of the 2-DoF manipulators subject to sever bit rate constraint

- The presentation of a new technique for remote monitoring and control of the 2-DoF robotic manipulators subject to sever computational constraint

The paper is organized as follows. In Section 2 we briefly describe our coding and control techniques presented in [16] and [17]; and we explain how they can be implemented to the 2-DoF robotic manipulator that we consider as the case study of the paper. In Section 3 using extensive computer simulations, we illustrate the satisfactory performances of these techniques for remote monitoring and control in the presence of severe communication imperfections. The paper is concluded in Section 4 by summarizing the main contributions of the paper and discussion on the future research directions.

Throughout certain conventions are used: $|\cdot|$ denotes the absolute value, $\|\cdot\|$ the Euclidean norm and V' denotes the transpose of vector/matrix V. A^{-1} and $\lambda_i(A)$ denote the inverse and eigenvalues of a square matrix A, respectively. '$\doteq$' means 'by definition is equivalent to' and $Z^t \doteq (Z_1, Z_2, ..., Z_t)$. $\mathbb{R}$ and $\mathbb{N}$ denote the sets of real numbers and natural numbers, respectively; and I is the identity matrix. Also, $x^{(i)}$ denotes the ith element of the vector X and $\underline{0}$ denotes the zero vector/matrix. $\mathbb{N}^+ \doteq \{0, 1, 2, 3, ...\}$ and $\mathbb{R}^+$ is the set of non-negative real numbers. B^+ denotes the Pseudo inverse of the matrix B.

2 Coding and Control Techniques for Reliable Remote Monitoring and Control

In this section we briefly describe the coding and control techniques proposed in [16] and [17] for remote monitoring and control subject to the random packet drop out and limited bit rate constraint and hence rate distortion imperfection. We also explain how they can be implemented to the robotic manipulator considered as the case study in this paper.

[16] and [17] were concerned with almost sure asymptotic tracking of the state trajectory as well as reference tracking of nonlinear dynamic systems over the packet erasure channel with feedback acknowledgment, which is an abstract model for communication via the Internet, WiFi and Zigbee modules (e.g., Digi XBee, Lora, Sigfox). Specifically, [16] and [17] were concerned with the block diagram of Fig. 1 described by the following nonlinear dynamic system and communication channel.

Dynamic System:

$$\begin{cases} X_{t+1} = F(X_t, U_t) \\ Y_t = X_t \end{cases} \tag{1}$$

where $t \in \mathbb{N}^+$ is the time instant, $F(X_t, U_t) \in \mathbb{R}^n$ is a smooth vector nonlinear function, $X_t \in \mathbb{R}^n$ is the vector of the states of the system, $Y_t \in \mathbb{R}^n$ is the observation output vector (sensor data) and $U_t \in \mathbb{R}^m$ is the control input vector. Note that the dynamic system (1) is a fully observable system as we assume $Y_t = X_t$. Throughout, it is assumed that the probability measure associated with the initial state X_0 with components $x_0^{(i)}$, $i = \{1, 2, ..., n\}$, has bounded support. That is, for each $i \in \{1, 2, ..., n\}$ there exists a compact set $[-L_0^{(i)}, L_0^{(i)}] \in \mathbb{R}$ such that $\Pr(x_0^{(i)} \in [-L_0^{(i)}, L_0^{(i)}]) = 1$. Note that X_0 is unknown for the remote decoder and controller.

Communication Channel: Communication channel between system and controller is a limited capacity erasure channel with feedback acknowledgment. It is a digital channel that transmits a packet of binary data in each channel use. The channel input and channel output alphabets are denoted by Z and $\tilde{Z}$, respectively; and Z_t denotes the channel input at time instant $t \in \mathbb{N}^+$, which is a packet of binary data with length R_t containing information bits. Let $\tilde{Z}_t$ be the channel output ad e denote the erasure symbol. Then,

$$\tilde{Z}_t = \begin{cases} Z_t & with\, probability\; 1-\alpha \\ e & with\, probability\; \alpha \end{cases} \tag{2}$$

That is, this channel erases a transmitted packet with probability α. Throughout, it is assumed that the erasure probability α is known a priori.

In the channel considered in this paper, there is a feedback acknowledgment from the receiver to the transmitter. That is, if a transmission is successful, an acknowledgment bit is sent from receiver to transmitter indicating that the transmission has been successful. The packet erasure channel with feedback acknowledgment is an abstract model for the commonly used data transmission technologies, such as the Internet and WiFi.

The objective of [16] and [17] were to design an encoder, decoder and a controller that resulted in almost sure asymptotic tracking of the state trajectory as well as reference tracking of the system (1), as defined below. These are also the objectives of this paper. For the 2-DoF robotic manipulator considered as the case study in this paper, we refer to the almost sure asymptotic tracking of the state trajectory as the tele-presence; and we refer to the almost sure asymptotic reference tracking as the tele-operation.

Definition 2.1 *(Almost Sure Asymptotic Tracking of the State Trajectory): Consider the block diagram of Fig. 1 described by the nonlinear dynamic system (1) over the packet erasure channel, as described above. It is said that the state trajectory is almost sure asymptotically tracked if and only if there exist an encoder, decoder and a controller such that the following property holds:* $\Pr(\lim_{t\to\infty} \|X_t - \hat{X}_t\| = 0) = 1$.

Definition 2.2 *(Almost Sure Asymptotic Reference Tracking): Consider the block diagram of Fig. 1 described by the nonlinear dynamic system (1) over the packet erasure channel, as described above. It is said that the system is almost sure asymptotically track the reference signal* $\mathcal{R}_t \in \mathbb{R}^n$ *if and only if there exist an encoder, decoder and a controller such that the following property holds:* $\Pr(\lim_{t\to\infty} \|X_t - \mathcal{R}_t\| = 0) = 1$.

Remark 2.3 *The above definitions for almost sure asymptotic tracking and reference tracking (for the case of* $\mathcal{R}_t = 0$*) were defined in [15] and latter on they have been used by others, e.g., [16], [17].*

In the following, we briefly describe the coding and control techniques that we proposed in [16] and [17] for almost sure asymptotic tracking and reference tracking of the nonlinear dynamic system (1) over the packet erasure channel. We then explain how they can be implemented on robotic manipulators.

2.1 Coding and Control Techniques of [16]

The proposed coding technique in [16] is based on the linearization method [20]. By implementing this method, we presented an encoder, decoder and a sufficient condition on the length of transmitted packets, R_t, at each linearization zone that guaranteed almost sure asymptotic state tracking of the family of the equivalent linear dynamic systems, which were resulted from the linearizing the nonlinear dynamic system (1). Note that as in each linearized zone we deal with a new linear dynamic system, the length of the transmitted packet is different in different linearized zones. Hence, we denote the length of transmitted packet in the linearized zone j by $R_{[j]}$. Having that, the proposed coding technique works as follows (for the simplicity of the presentation consider the scalar case).

At the time instant $t = 0$, we notice that $X_0 \in [-L_0, L_0]$, where the upper bound L_0 is known for both encoder and decoder; and we fix the rate to be $\bar{R}_{[0]}$. Then, using the coding technique that will be described very shortly, the reconstruction of X_0 denoted by $\hat{\hat{X}}_0$ is obtained at the decoder. Due to the existence of the feedback acknowledgment, the encoder also reconstructs $\hat{\hat{X}}_0$. Then, at this time instant ($t = 0$), the encoder and decoder linearize the nonlinear dynamic system at the working point $(\hat{\hat{X}}_0, U_0)$, $U_0 = 0$, which results in a state space system matrix $A_{[0]}$ and $B_{[0]}$ for the equivalent linear model. Then, the encoder and decoder partition the interval $[-L_0, L_0]$ into $2^{R_{[0]}}$ equal sized, non-overlapping sub-intervals and the center of each sub-interval is chosen as the index of that interval $(\gamma_0, \gamma_1, ..., \gamma_{2^{R_{[0]}}-1})$. Subsequently, the index of the sub-interval that includes X_0 (e.g., γ_{j0} where $j0 \in \{0, 1, ..., 2^{R_{[0]}} - 1\}$) is encoded into $R_{[0]}$ bits and transmitted to the decoder through the packet erasure channel. If the decoder receives this $R_{[0]}$ bits successfully, it identifies the index of the sub-interval where X_0 lives in; and the value of this index is chosen as $\hat{X}_0$. Therefore, the decoding error for this case is bounded above by $|X_0 - \hat{X}_0| \leq V_0 = \frac{L_0}{2^{R_{[0]}}}$. But if erasure occurs, then $\hat{X}_0 = 0$; and therefore, $|X_0 - \hat{X}_0| \leq V_0 = L_0$. Hence, the decoding error can be represented as follows:

$$|E_0| \doteq |X_0 - \hat{X}_0| \leq V_0 = M_0 L_0;$$

$$M_0 = \begin{cases} \frac{1}{2^{R_{[0]}}}, & \Pr(M_0 = \frac{1}{2^{R_{[0]}}}) = 1 - \alpha \\ 1, & \Pr(M_0 = 1) = \alpha \end{cases} \tag{3}$$

Note that $\hat{\hat{X}}_0$ is constructed similarly by implementing $\bar{R}_{[0]}$ bits. The procedure for the reconstruction of $\hat{\hat{X}}_0$ may be repeated several times until we have a successful transmission for the reconstruction of $\hat{\hat{X}}_0$. At the time instant $t = 1$, the encoder encodes $X_1 - A_{[0]}\hat{X}_0 - B_{[0]}U_0$. To encode this signal, the interval $[-L_1, L_1]$ is calculated as follows:$|X_1 - A_{[0]}\hat{X}_0 - B_{[0]}U_0| = |A_{[0]}X_0 - A_{[0]}\hat{X}_0| = |A_{[0]}||X_0 - \hat{X}_0| \leq |A_{[0]}|V_0 = L_1$. Then, the encoder and decoder partition the interval $[-L_1, L_1]$ into $2^{R_{[0]}}$ equal sized, non-overlapping sub-intervals and the center of each sub-interval is chosen as the index of that interval. When the encoder observes the signal $X_1 - A_{[0]}\hat{X}_0 - B_{[0]}U_0$, the index of the sub-interval that includes $X_1 - A_{[0]}\hat{X}_0 - B_{[0]}U_0$ (e.g., γ_{j1} where $j1 \in \{0, 1, ..., 2^{R_{[0]}} - 1\}$) is encoded into $R_{[0]}$ bits and transmitted to the decoder through the packet erasure channel. Subsequently, the decoder constructs $\hat{X}_1$ as follows: $\hat{X}_1 = \gamma_{j1} + A_{[0]}\hat{X}_0 + B_{[0]}U_0$, if $M_1 = \frac{1}{2^{R_{[0]}}}$ with the probability of $\Pr(M_1 = \frac{1}{2^{R_{[0]}}}) = 1 - \alpha$; and $\hat{X}_1 = A_{[0]}\hat{X}_0 + B_{[0]}U_0$, if $M_1 = 1$ with the probability of $\Pr(M_1 = 1) = \alpha$. Therefore,

$$|E_1| \doteq |X_1 - \hat{X}_1| \leq V_1 = M_1 L_1;$$

$$M_1 = \begin{cases} \frac{1}{2^{R_{[0]}}}, & \Pr(M_1 = \frac{1}{2^{R_{[0]}}}) = 1 - \alpha \\ 1, & \Pr(M_1 = 1) = \alpha \end{cases} \tag{4}$$

For the next step ($t = 2$), if $|E_1| \leq |E_0|$, this procedure continues with the equivalent state space matrices $A_{[0]}$ and $B_{[0]}$ and the packet length $R_{[0]}$; but if $|E_1| > |E_0|$, then the encoder linearizes the nonlinear dynamic system at the new working point $(\hat{X}_1, U_1)$ that results in the state space system matrices $A_{[1]}$ and $B_{[1]}$ of the equivalent linear model (i.e., the system (5) with $j = 1$). The encoder by sending $R_{[1]} \neq R_{[0]}$ bits through the packet erasure channel informs the decoder that a new linearization has been applied. Therefore, the decoder performs the same linearization; and the rest of the procedure continues with the new matrices $A_{[1]}$ and $B_{[1]}$.

$$\begin{cases} X_{t+1} = A_{[0]}X_t + B_{[0]}U_t; \ t \in [0, t_1), \\ X_{t+1} = A_{[1]}X_t + B_{[1]}U_t; \ t \in [t_1, t_2) \\ \vdots \\ X_{t+1} = A_{[j]}X_t + B_{[j]}U_t; \ t \in [t_j, t_{j+1}), \quad j \in N_+ \\ Y_t = X_t \end{cases} \tag{5}$$

By following a similar procedure, as described above, the sequence $\hat{X}_0, \hat{X}_1, \hat{X}_0, ...$ are constructed at the decoder. The vector case ($X_t \in \mathbb{R}^n$) was treated similarly in [16]. It has been proved in [16] that if $\triangle t_j \doteq t_{j+1} - t_j$ ($j \in N_+$)s are sufficiently large and the packet lengths $R_t = R_{[j]}$ ($t \in [t_j, t_{j+1})$) satisfy the following inequalities:

$$(1 - \alpha)R_{[j]} > \sum_{i=1}^{n} \max\{0, \log_2 |\lambda_i(A_{[j]})|\}; \ \forall j \in \mathbb{N}_+, \tag{6}$$

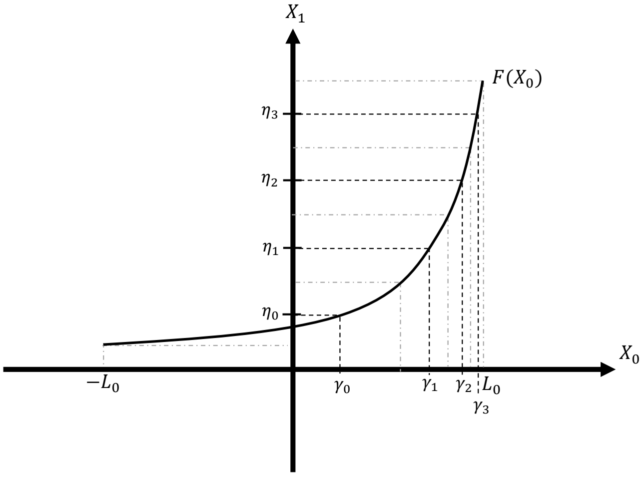

Fig. 3. Equal sized, non-overlapping sub-intervals for encoding with rate $R = 2$ using the coding technique of [17]

then using the above coding technique we have almost sure asymptotic state tracking. Note that the first condition (i.e., $\triangle t_j \doteq t_{j+1} - t_j$ for $j \in \mathbb{N}_+$ is sufficiently large) is satisfied if the sampling period is small compared with the linearization period.

Now, for the nonlinear system (1) suppose that for each linearized equivalent system, there exists a matrix $K_{[j]}$ such that the matrix $A_{[j]} + B_{[j]}K_{[j]}$ is a stable matrix (e.g., $K_{[j]} = -B^+_{[j]}A_{[j]}$, where $B^+_{[j]}$ is the Pseudo inverse). Then, using the proposed coding technique and the controller $U_t = K_{[j]}\hat{\hat{X}}_t + W_{[j],t}$ where $W_{[j],t} \doteq -B^+_{[j]}(A_{[j]}\mathcal{R}_t - \mathcal{R}_{t+1})$ and $\hat{\hat{X}}_t \doteq \hat{X}_t - \mathcal{R}_t$ for each linearized system, we have almost sure asymptotic reference tracking [16].

Remark 2.4 *The input to the family of the linearized systems (5) is the vector* U_t*, as given above, which involves* $\hat{X}_t$*.* $\hat{X}_t$ *is the decoder output. And the encoder and decoder compensate the imperfections due to the transmission of system measurements over the packet erasure channel, which is an abstract model for the transmission over the Internet and WiFi communication links.*

2.2 Coding and Control Techniques of [17]

The coding and control techniques of [17] work differently. The coding and control techniques of [17] are not based on the linearization method and throughout we transmit with a fixed rate R rather than a variable rate $R_{[j]}$. [17] assumes the nonlinear dynamic system $F(X_t, U_t)$ is the control affine, that is, $F(X_t, U_t) = F(X_t) + BU_t$, where $F(.)$ is a piece wise non-decreasing or non-increasing function (see Fig. 3). The coding technique of [17] is similar to the coding technique of [16] for each linearized zone; except it considers the following dynamic $X_{t+1} = F(X_t) + BU_t$ and instead of encoding γ_j it encodes $\eta_j = F^{-1}(\gamma_j)$. It has been proved in [17] that under some mild conditions on the transmission rate R, the proposed coding technique results in the almost sure asymptotic tracking of the state trajectory. It has been also proved that the control vector $U_t = -B^+(F(\hat{X}_t) - \mathcal{R}_{t+1})$ results in the almost sure asymptotic reference tracking.

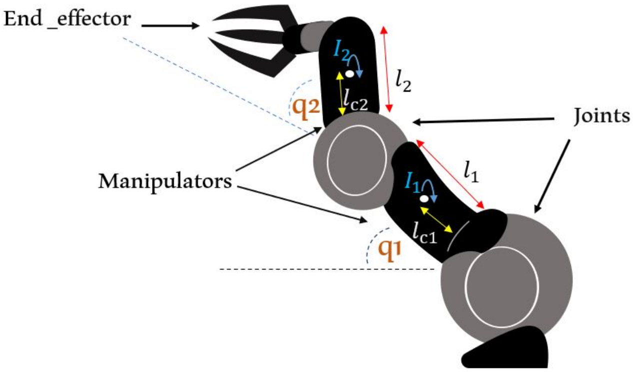

Fig. 4. The robotic manipulator considered as the case study of the paper

2.3 Applications of the Proposed Techniques on Two-Link Robotic Manipulators

Now, we implement these coding and control techniques to the case study of the paper, which is a two-link robotic manipulator shown in Fig. 4. This type of manipulators are very common in manufacturing industries. Its dynamic is described by the following equation [20] (for the simplicity of the presentation, we drop the continuous time dependency index).

$$H(q)\ddot{q} + C(q,\dot{q})\dot{q} + g(q) = \tau, \tag{7}$$

where

$$H(q) = \begin{pmatrix} H_{11} & H_{12} \\ H_{21} & H_{22} \end{pmatrix}, \ \ddot{q} = \begin{pmatrix} \ddot{q}_1 \\ \ddot{q}_2 \end{pmatrix},$$

$$C(q,\dot{q}) = \begin{pmatrix} -h\dot{q}_2 & -h\dot{q}_1 - h\dot{q}_2 \\ h\dot{q}_1 & 0 \end{pmatrix}, \ \dot{q} = \begin{pmatrix} \dot{q}_1 \\ \dot{q}_2 \end{pmatrix},$$

$$g(q) = \begin{pmatrix} g_1 \\ g_2 \end{pmatrix}, \quad \tau = \begin{pmatrix} \tau_1 \\ \tau_2 \end{pmatrix},$$

where

$$H_{11} = m_1 l_{C1}^2 + I_1 + m_2[l_1^2 + l_{C2}^2 + 2l_1 l_{C2}\cos(q_2)] + I_2$$
$$H_{22} = m_2 l_{C2}^2 + I_2$$
$$H_{21} = H_{12} = m_2 l_1 l_{C2}\cos(q_2) + I_2 + m_2 l_{C2}^2$$
$$h = m_2 l_1 l_{C2}\sin(q_2)$$
$$g_1 = m_1 l_{C1} g\cos(q_1) + m_2 g[l_{C2}\cos(q_1 + q_2) + l_1\cos(q_1)]$$
$$g_2 = m_2 l_{C2} g\cos(q_1 + q_2),$$

and m_1 is the mass of the fist arm, m_2 is the mass of the second arm and g is the earth gravity acceleration coefficient (i.e., g =9.81).
In order to implement the coding and control techniques of [16] and [17] to the above manipulator, it is required that we rewrite the above dynamic in the state space form. To do that, we define the following states:

$$x^{(1)} = q_1,\ x^{(2)} = q_2,\ x^{(3)} = \dot{q}_1,\ x^{(4)} = \dot{q}_2.$$

Subsequently, we have the following state space representation for the above manipulator:

$$\begin{aligned}
\dot{x}^{(1)} &= x^{(3)} \\
\dot{x}^{(2)} &= x^{(4)} \\
\dot{x}^{(3)} &= \frac{num_3}{H_{12}H_{21} - H_{11}H_{22}} \\
num_3 &= \tau_2 H_{12} - \tau_1 H_{22} - g_2 H_{12} - hH_{12}{x^{(3)}}^2 - hH_{22}{x^{(4)}}^2 \\
&\quad + g_1 H_{22} - 2hH_{22}x^{(3)}x^{(4)} \\
\dot{x}^{(4)} &= \frac{num_4}{H_{22}H_{11} - H_{21}H_{12}} \\
num_4 &= \tau_2 H_{11} - \tau_1 H_{21} - g_2 H_{11} - hH_{11}{x^{(3)}}^2 - hH_{21}{x^{(4)}}^2 \\
&\quad + g_1 H_{21} - 2hH_{21}x^{(3)}x^{(4)}.
\end{aligned}$$

The measurement data from this robotic manipulator is the vector Y and the control commands is the vector U described as follows:

$$Y = \begin{pmatrix} x^{(1)} \\ x^{(2)} \\ x^{(3)} \\ x^{(4)} \end{pmatrix},\ U = \begin{pmatrix} \tau_1 \\ \tau_2 \end{pmatrix}.$$

Because the communication network is a digital channel, we need to sample the measurement data with a fixed period of T seconds and apply the control commands via the so called Zero Order Hold (ZOH) [21] with the update period of T seconds. Hence, in the block diagram of Fig. 1 we should deal with the following equivalent discrete time dynamic system for the above manipulator for the implementation of the coding and control techniques of [16] and [17]. The following equivalent discrete time model is obtained by implementing the Euler's approximation method [21]:

$$\begin{aligned}
x^{(1)}_{t+1} &= Tx^{(3)}_t + x^{(1)}_t \doteq f^{(1)} \\
x^{(2)}_{t+1} &= Tx^{(4)}_t + x^{(2)}_t \doteq f^{(2)} \\
x^{(3)}_{t+1} &= T\left(\frac{num_3}{H_{12}H_{21} - H_{11}H_{22}}\right) + x^{(3)}_t \doteq f^{(3)} \\
x^{(4)}_{t+1} &= T\left(\frac{num_4}{H_{22}H_{11} - H_{21}H_{12}}\right) + x^{(4)}_t \doteq f^{(4)}
\end{aligned}$$

Hence, the matrices $A_{[j]}$ and $B_{[j]}$ for the jth linearized system to be used in the coding and control techniques of [16] are given by the following matrices.

$$\begin{aligned}
A_{[j]} &= \begin{pmatrix}
\frac{\partial f^{(1)}}{\partial x^{(1)}} & \frac{\partial f^{(1)}}{\partial x^{(2)}} & \frac{\partial f^{(1)}}{\partial x^{(3)}} & \frac{\partial f^{(1)}}{\partial x^{(4)}} \\
\frac{\partial f^{(2)}}{\partial x^{(1)}} & \frac{\partial f^{(2)}}{\partial x^{(2)}} & \frac{\partial f^{(2)}}{\partial x^{(3)}} & \frac{\partial f^{(2)}}{\partial x^{(4)}} \\
\frac{\partial f^{(3)}}{\partial x^{(1)}} & \frac{\partial f^{(3)}}{\partial x^{(2)}} & \frac{\partial f^{(3)}}{\partial x^{(3)}} & \frac{\partial f^{(3)}}{\partial x^{(4)}} \\
\frac{\partial f^{(4)}}{\partial x^{(1)}} & \frac{\partial f^{(4)}}{\partial x^{(2)}} & \frac{\partial f^{(4)}}{\partial x^{(3)}} & \frac{\partial f^{(4)}}{\partial x^{(4)}}
\end{pmatrix} |_{(\hat{X}_{t_j}, U_{t_j})} \\
&= \begin{pmatrix}
1 & 0 & T & 0 \\
0 & 1 & 0 & T \\
a_{31} & a_{32} & a_{33} & a_{34} \\
a_{41} & a_{42} & a_{43} & a_{44}
\end{pmatrix} |_{(\hat{X}_{t_j}, U_{t_j})},
\end{aligned}$$

$$\begin{aligned}
a_{31} &= \frac{1}{H_{11}H_{22} - H_{12}H_{21}}\left(\frac{\partial g_2}{\partial q_1}H_{12} - \frac{\partial g_1}{\partial q_1}H_{22}\right) \\
a_{32} &= \frac{\partial f_3}{\partial q_2} \\
a_{33} &= \frac{T.2H_{12}hx^{(3)} + T.2H_{22}hx^{(4)}}{H_{11}H_{22} - H_{12}H_{21}} + 1 \\
a_{34} &= \frac{T.2H_{22}h(x^{(3)} + x^{(4)})}{H_{11}H_{22} - H_{12}H_{21}} \\
a_{41} &= \frac{-1}{H_{11}H_{22} - H_{12}H_{21}}\left(\frac{\partial g_2}{\partial q_1}H_{11} - \frac{\partial g_1}{\partial q_1}H_{21}\right) \\
a_{42} &= \frac{\partial f_4}{\partial q_2} \\
a_{43} &= \frac{-T.2H_{11}hx^{(3)} - T.2H_{21}hx^{(4)}}{H_{11}H_{22} - H_{12}H_{21}} \\
a_{44} &= 1 - \frac{T.2H_{21}h(x^{(3)} + x^{(4)})}{H_{11}H_{22} - H_{12}H_{21}}.
\end{aligned}$$

$$\begin{aligned}
B_{[j]} &= \begin{pmatrix}
\frac{\partial f^{(1)}}{\partial \tau_1} & \frac{\partial f^{(1)}}{\partial \tau_2} \\
\frac{\partial f^{(2)}}{\partial \tau_1} & \frac{\partial f^{(2)}}{\partial \tau_2} \\
\frac{\partial f^{(3)}}{\partial \tau_1} & \frac{\partial f^{(3)}}{\partial \tau_2} \\
\frac{\partial f^{(4)}}{\partial \tau_1} & \frac{\partial f^{(4)}}{\partial \tau_2}
\end{pmatrix} |_{(\hat{X}_{t_j}, U_{t_j})} \\
&= \begin{pmatrix}
0 & 0 \\
0 & 0 \\
\frac{TH_{22}}{H_{11}H_{22} - H_{12}H_{21}} & \frac{-TH_{12}}{H_{11}H_{22} - H_{12}H_{21}} \\
\frac{-TH_{21}}{H_{11}H_{22} - H_{12}H_{21}} & \frac{TH_{11}}{H_{11}H_{22} - H_{12}H_{21}}
\end{pmatrix} |_{(\hat{X}_{t_j}, U_{t_j})}.
\end{aligned}$$

Following that a linear controller for each linearized zone in the form of $U_t = -B^{+}_{[j]}A_{[j]}\hat{\tilde{\hat{X}}}_t + W_{[j],t}$, $W_{[j],t} = -B^{+}_{[j]}(A_{[j]}\mathcal{R}_t - \mathcal{R}_{t+1})$, $\hat{\tilde{\hat{X}}}_t = \hat{X}_t - \mathcal{R}_t$ is obtained for the tele-operation of the two-link manipulator.

Now, let $X_t = \begin{pmatrix} x_t^{(1)} \\ x_t^{(2)} \\ x_t^{(3)} \\ x_t^{(4)} \end{pmatrix}$, $\hat{X}_t = \begin{pmatrix} \hat{x}_t^{(1)} \\ \hat{x}_t^{(2)} \\ \hat{x}_t^{(3)} \\ \hat{x}_t^{(4)} \end{pmatrix}$ (which is the decoder output), $d_1 = \bar{H}_{12}\bar{H}_{21} - \bar{H}_{11}\bar{H}_{22}$ and $d_2 = \bar{H}_{22}\bar{H}_{11} - \bar{H}_{21}\bar{H}_{12}$, where

$$\begin{aligned}
&\bar{H}_{11} = m_1 l_{C1}^2 + I_1 + m_2[l_1^2 + l_{C2}^2 + 2l_1 l_{C2}\cos(x_t^{(2)})] + I_2 \\
&\bar{H}_{22} = m_2 l_{C2}^2 + I_2 \\
&\bar{H}_{21} = \bar{H}_{12} = m_2 l_1 l_{C2}\cos(x_t^{(2)}) + I_2 + m_2 l_{C2}^2 \\
&\bar{h} = m_2 l_1 l_{C2}\sin(x_t^{(2)}) \\
&\bar{g}_1 = m_1 l_{C1} g\cos(x_t^{(1)}) + m_2 g[l_{C2}\cos(x_t^{(1)} + x_t^{(2)}) \\
&+ l_1\cos(x_t^{(1)})] \\
&\bar{g}_2 = m_2 l_{C2} g\cos(x_t^{(1)} + x_t^{(2)}).
\end{aligned}$$

Let also $F(X_t) = \begin{pmatrix} f^{(1)} \\ f^{(2)} \\ \bar{f}^{(3)} \\ \bar{f}^{(4)} \end{pmatrix}$, where

$$\begin{aligned}
&\bar{f}^{(3)} = \frac{num_5}{d_1}, \\
&num_5 = -\bar{g}_2\bar{H}_{12} - \bar{h}\bar{H}_{12}{x_t^{(3)}}^2 - \bar{h}\bar{H}_{22}{x_t^{(4)}}^2 + \bar{g}_1\bar{H}_{22} \\
&-2\bar{h}\bar{H}_{22}x_t^{(3)}x_t^{(4)} \\
&\bar{f}^{(4)} = \frac{num_6}{d2}, \\
&num_6 = -\bar{g}_2\bar{H}_{11} - \bar{h}\bar{H}_{11}{x_t^{(3)}}^2 - \bar{h}\bar{H}_{21}{x_t^{(4)}}^2 + \bar{g}_1\bar{H}_{21} \\
&-2\bar{h}\bar{H}_{21}x_t^{(3)}x_t^{(4)}.
\end{aligned}$$

Also, let

$$\bar{B} = \begin{pmatrix} 0 & 0 \\ 0 & 0 \\ -\frac{\bar{H}_{22}}{d_1} & \frac{\bar{H}_{12}}{d_1} \\ -\frac{\bar{H}_{21}}{d_2} & \frac{\bar{H}_{11}}{d_2} \end{pmatrix}.$$

Then, the nonlinear controller equipped with the coding technique of [17] that results in the tele-operation of the two-link manipulator is given by

$$U_t = -\bar{B}^{+}(F(\hat{X}_t) - \mathcal{R}_{t+1}).$$

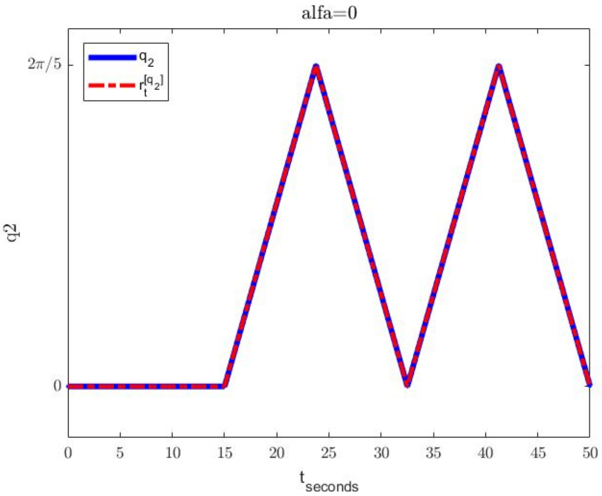

Fig. 5. The reference signal and the trajectory taken by the manipulator for q_2 when the reference trajectory is non-smooth, $\alpha = 0$, $T = 0.01$ and the coding and control techniques of [16] are used

3 Simulation Results

In this section we evaluate the performances of the proposed coding and control techniques applied to the case study of the paper in the presence of severe communication imperfections, which are common in the industrial environments. For the simulation purposes we choose the following parameters for the two-link manipulator of Fig. 4, which is the case study of the paper. These parameters were borrowed from [22]. Table 1 presents the parameters of the manipulator for the actual case (i.e., when its end-effector carries a pre-defined load) as well as the nominal case (i.e., when its end-effector does not carry any load). Note that the coding and control techniques are designed based on the nominal and actual dynamics following the status of the end-effector of the manipulator of the case study.

Table 1
Actual And Nominal Parameters

Parameter	Actual	Nominal
m_1	4 Kg	3.2 Kg
m_2	2 Kg	2.4 Kg
l_1	0.5 m	0.5 m
l_2	0.25 m	0.25 m
l_{C1}	0.25 m	0.3 m
l_{C2}	0.15 m	0.1 m
I_1	1 $Kg\ m^2$	1.2 $Kg\ m^2$
I_2	0.8 $Kg\ m^2$	0.6 $Kg\ m^2$

Throughout this section it is assumed that the torques, which are applied on the manipulator joints are subject to operational constraints. That is, $|\tau_1| \leq 6.4 N.m$ and $|\tau_2| \leq 2.9 N.m$. Also, the rate of change of torques for $T = 0.01$ is limited up to 0.03 $N.m$ (for $T = 0.1$ it is therefore limited up to 0.3 $N.m$). We also set $L_0^{(1)} = \frac{\pi}{6}$, $L_0^{(2)} = \frac{\pi}{100}$ and $\dot{q}_1(0) = \dot{q}_2(0) = 0$ (therefore, $L_0^{(3)} =$

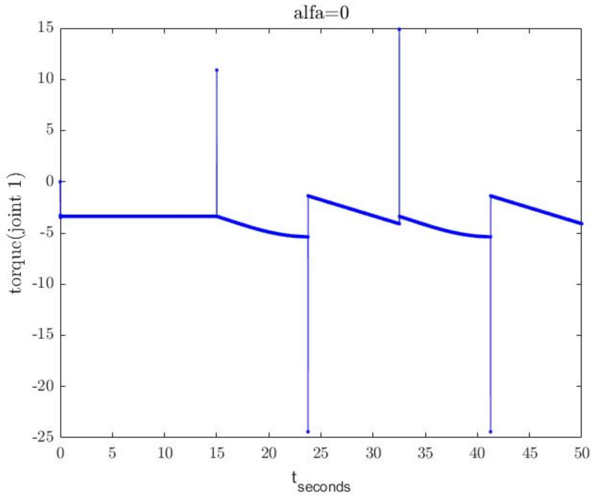

Fig. 6. The required torque for joint 1 when reference trajectories are non-smooth, $\alpha = 0$, $T = 0.01$ and the coding and control techniques of [16] are used

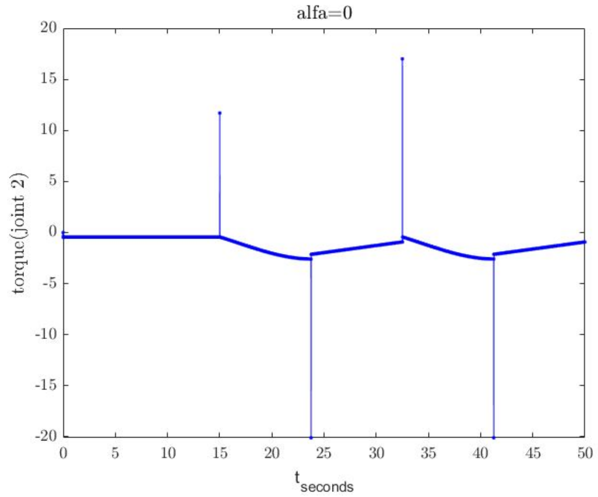

Fig. 7. The required torque for joint 2 when reference trajectories are non-smooth, $\alpha = 0$, $T = 0.01$ and the coding and control techniques of [16] are used

$L_0^{(4)} = 0$). We also set $X_0 = \underline{0}$ for simulations. Moreover, for the coding and control techniques of [16] we set $\bar{R}_{[0]} = 22$ and for those of [17] we set $\bar{R} = 6$. Note that for the remote reference tracking, q_1, q_2, $\dot{q}_1$ and $\dot{q}_2$ are sampled with the sample period of T seconds and transmitted to the remote controller.

3.1 The Performance under the Coding and Control Techniques of [16]

Under the above conditions, for the case of $\alpha = 0$ and $T = 0.01$ we implement the aforementioned coding and control techniques of [16]to track the reference signals for q_1, which is $\frac{\pi}{8}$, and q_2 as shown in Fig. 5 by dashed trajectory. For the time interval of 0 to 15 seconds the nominal dynamic is simulated and for the interval of 15 to 23.75 seconds the actual dynamic is simulated, then for the time interval of 23.75 to 32.5 the nominal dynamic is simulated and for the next time interval of 32.5 to 41.25 the actual dynamic is simulated and so on and so forth. That is, the manipulator frequently picks up a pre-defined object and moves it and then returns to pick up and move another similar object. When it carries this object, its dynamic is described by the actual dynamic and when it returns to pick up another similar object, its dynamic is the nominal dynamic. This is a typical scenario for the robotic manipulator of the case study as it very often moves a pre-defined load and after dropping this load, it returns to its initial position to pick up, move and drop another similar load. Fig. 5 also illustrates the trajectory for q_2 taken by the manipulator (solid line). As it is clear from this figure we have an excellent quality of the reference tracing. We have similar

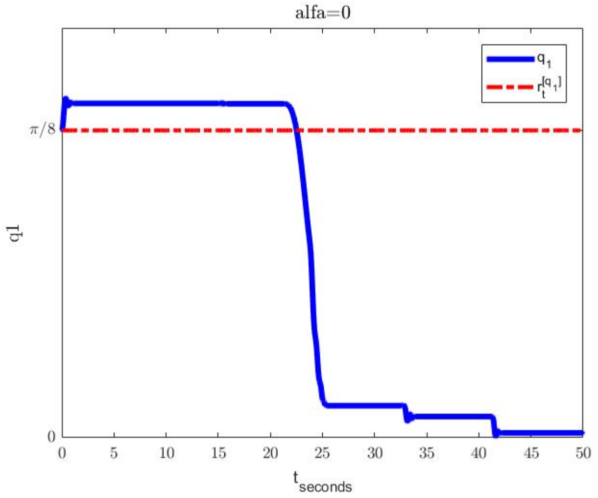

Fig. 8. The reference signal and the trajectory taken by the manipulator for q_1 subject to the the operational constraints when reference trajectories are non-smooth, $\alpha = 0$, $T = 0.01$ and the coding and control techniques of [16] are used

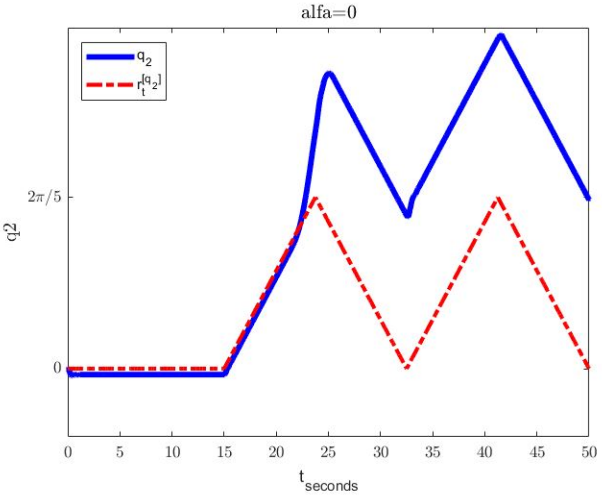

Fig. 9. The reference signal and the trajectory taken by the manipulator for q_2 subject to the operational constraints when reference trajectories are non-smooth, $\alpha = 0$, $T = 0.01$ and the coding and control techniques of [16] are used

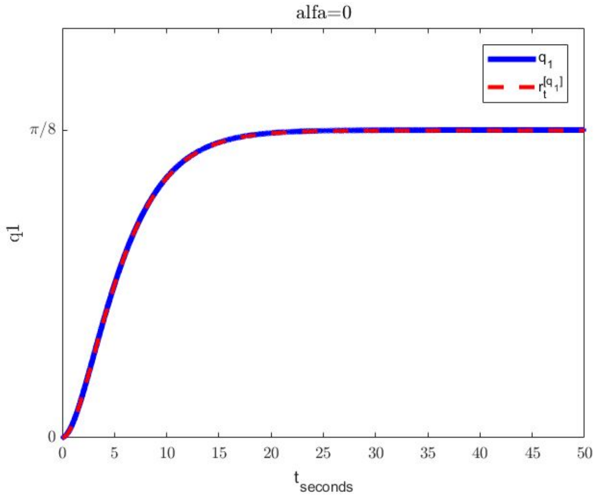

Fig. 10. The smooth version of the reference signal and the trajectory taken by the manipulator for q_1 when $\alpha = 0$, $T = 0.01$ and the coding and control techniques of [16] are used

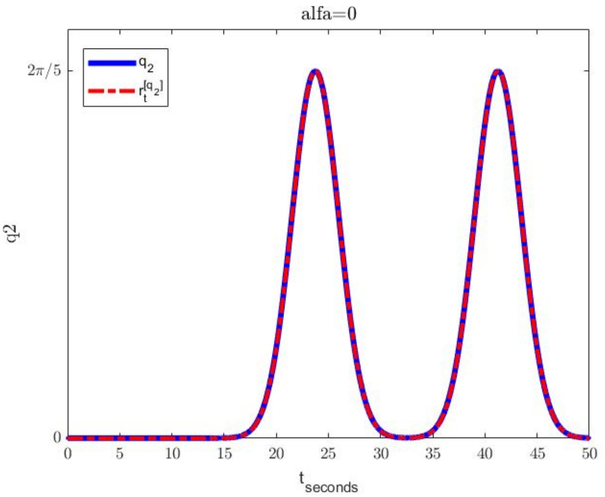

Fig. 11. The smooth version of the reference signal and the trajectory taken by the manipulator for q_2 when $\alpha = 0$, $T = 0.01$ and the coding and control techniques of [16] are used

excellent quality of reference tracking for q_1. But, this excellent quality comes with a price. Fig. 6 and Fig. 7 illustrate the required torques for this reference tracking. Due to the operational constrains the robotic manipulator of the case study obviously is not able to execute these required torques; and what we get are the results reported in Fig. 8 and Fig. 9.

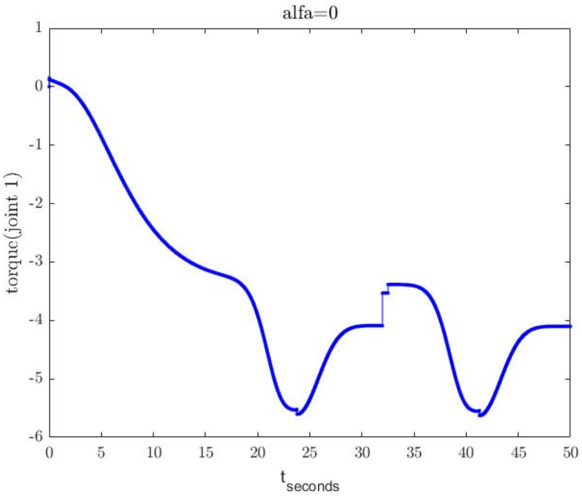

Fig. 12. The required torque for joint 1 when reference trajectories are smooth, $\alpha = 0$, $T = 0.01$ and the coding and control techniques of [16] are used

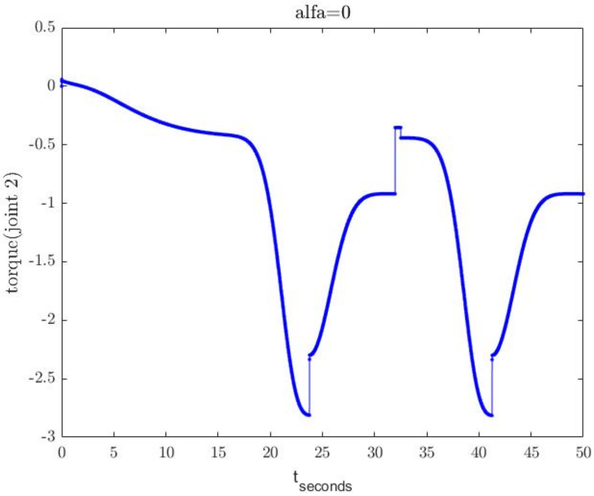

Fig. 13. The required torque for joint 2 when reference trajectories are smooth, $\alpha = 0$, $T = 0.01$ and the coding and control techniques of [16] are used

Now, in order to satisfy the operational constrains, we implement the smooth version of the reference signals as they are shown in Fig. 10 and Fig. 11. Fig. 12 and Fig. 13 illustrate the required torques for having this excellent quality of the reference tracking. As it is clear from these figures, by smoothing the reference signals, the upper bound constraints on torques are satisfied; but the rate constraints are not satisfied. Nevertheless, when these torques are applied by the manipulator to its joints by considering the rate and the upper bound constraints, we get a very similar result for the reference tracking as shown in Fig. 10 and Fig. 11 with the applied torques shown by Fig. 14 and Fig. 15. This indicates that our modified method, which is based on smoothing the reference signal results in a satisfactory performance. Note that whenever the value of the required torque passes the upper bound constraint, the upper bound is applied by the manipulator. Similarly, when the rate of change of torque passes its bound, the rate of change of torque is limited to the plus or the minus of the maximum allowable rate of change of torque (e.g., ± 0.03 for $T = 0.01$). Now, we evaluate the tele-presence and tele-operation performances in the presence of severe random packet drop out with the erasure probability of $\alpha \in [0, 1)$. That is, when sensor data is not received at the destination with the probability of $\alpha.100\%$. For the fair comparison,

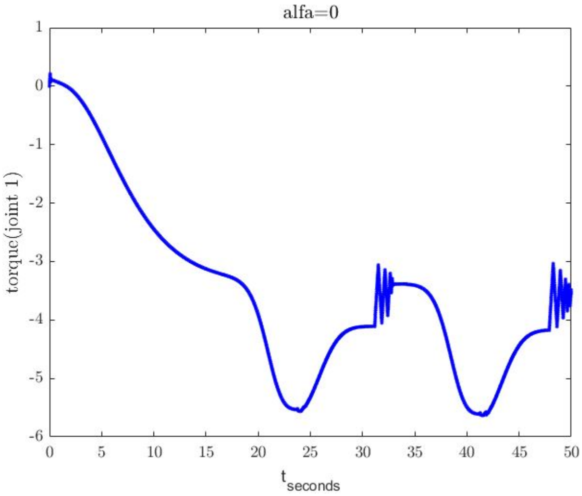

Fig. 14. The applied torque on joint 1 by considering the operational constraints when reference trajectories are smooth, $\alpha = 0$, $T = 0.01$ and the coding and control techniques of [16] are used

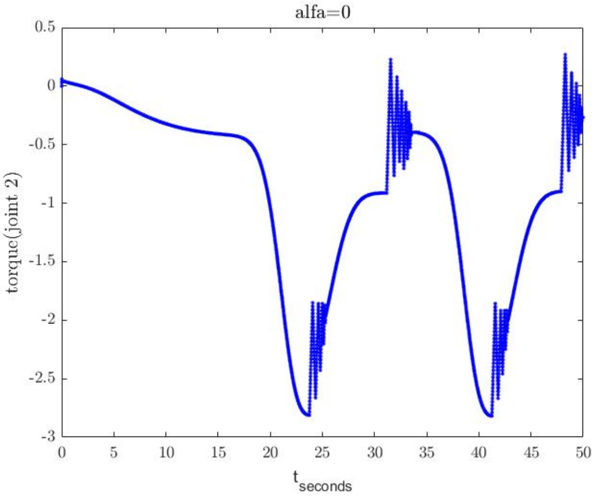

Fig. 15. The applied torque on joint 2 by considering the operational constraints when reference trajectories are smooth, $\alpha = 0$, $T = 0.01$ and the coding and control techniques of [16] are used

we define the following Root Sum Square Error (RSSE) criterion [17]:

$$RSEE = \sqrt{\sum_{t=0}^{t=50/T} ((x_t^{(1)} - r_t^{(1)})^2 + (x_t^{(2)} - r_t^{(2)})^2)}.$$

For the case of $T = 0.01$ seconds and $\alpha = 0$ (Fig. 10 to Fig. 15), $RSSE = 0.0568$ (without considering the operational constraints) and $RSSE^* = 1.5921$ (by considering the operational constraints). For the other cases, the $RSSE$s are reported in Table 2. Table 2 indicates that even for the extremely severe communication imperfections, the quality of the reference tracking is as excellent as the case of $\alpha = 0$. Nevertheless, this comes with a price for the severe cases. While for very small α, the length of transmitted packets is 4 or 5 bits, for $\alpha = 0.99$, this number is 20 or 21 bits.

Table 2
$RSSE$s for $T = 0.01$ when the coding and control techniques of [16] are used. $RSSE$: Without considering the operational constraints. $RSSE^*$: By considering the operational constraints.

α	$RSSE$	$RSSE^*$
0	0.0568	1.5921
0.1	0.0562	1.5628
0.2	0.0584	1.5752
0.5	0.0562	1.5631
0.75	0.059	1.5630
0.9	0.0562	1.5342
0.99	0.0568	1.5630

It is desirable to increase the sampling period to increase the life time of the processors and also be able to use cheaper processors. Nevertheless, it has been shown in [16] for autonomous vehicles that by increasing the sampling period the quality of the reference tracking is getting worse. This is a direct consequence of the stability requirement of switching systems as discussed in [16]. For the case of $\alpha = 0.5$, the effects of different sampling periods in $RSSE$ are reported in Table 3. From Table 3, it is clear that by increasing the sampling period, the quality of the reference tracking is getting worse, as it is expected.

Table 3
RSSE for $\alpha = 0.5$ when the coding and control techniques of [16] are used.

T	$RSSE$
0.01	0.0562
0.1	0.5616
0.2	1.1256
0.5	2.8701
1	6.0510
2	13.3120

3.2 The Performance of the Coding and Control Techniques of [17]

Computer simulation illustrates that the coding and control techniques of [17] for the reference trajectories, as shown in Fig. 10 and Fig. 11, are not able to satisfy the bound constraints on torques. Therefore, throughout this section, we focus on the reference trajectories as shown in Fig. 16 for q_2 and $\frac{\pi}{2}$ for q_1. Fig. 17 and Fig. 18 illustrate the applied torques on manipulator joints for tracking these reference trajectories. Note that the coding and control techniques of [17] can not satisfy the

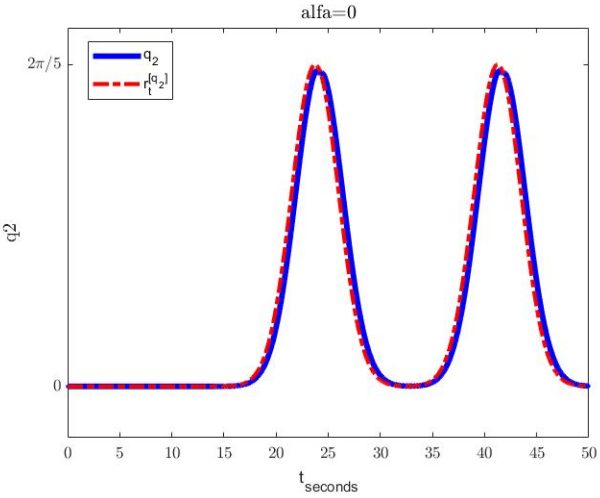

Fig. 16. The smooth version of the reference signal and the trajectory taken by the manipulator for q_2 when $\alpha = 0$, $T = 0.01$ and the coding and control techniques of [17] are used

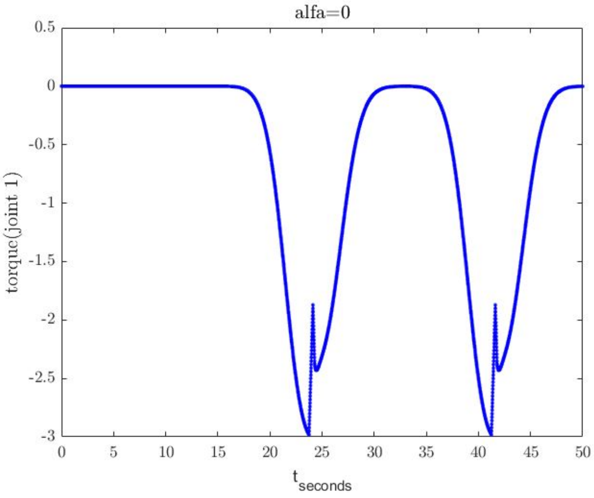

Fig. 17. The applied torque on joint 1 by considering the operational constraints when reference trajectories are smooth, $\alpha = 0$, $T = 0.01$ and the coding and control techniques of [17] are used

bound constraints on torques for the reference trajectories as shown in Fig. 10 and Fig. 11; and the coding and control techniques of [16] cannot also satisfy the bound constraints on torques for the reference trajectories as shown above.

Table 4 and Table 5 are the counterparts of Table 2 and Table 3 for the above reference trajectories when different α s and sample periods are implemented.

4 Conclusion and Future Research Direction

In this paper we illustrated the applications of the coding and control techniques of [16] and [17] in the telepresence and tele-operation of the 2-DoF robotic manipulators over the packet erasure channel. It has been illustrated that these techniques result in satisfactory performances even in the presence of sever communication imperfections provided the bound constraints on applied torques is satisfied. The techniques presented in [16] provides a slightly better tracking performance compared to the other technique presented in [17]; but it requires frequent model updates, higher bit rate and variable bit rate.

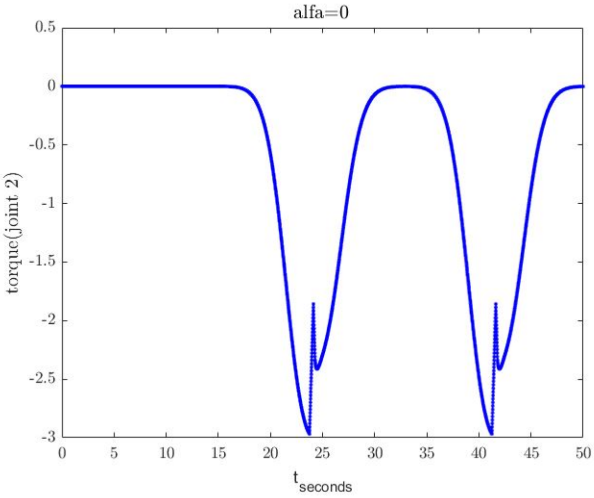

Fig. 18. The applied torque on joint 2 by considering the operational constraints when reference trajectories are smooth, $\alpha = 0$, $T = 0.01$ and the coding and control techniques of [17] are used

Table 4
$RSSE$s for $T = 0.01$ when the coding and control techniques of [17] are used. $RSSE$: Without considering the operational constraints. $RSSE^*$: By considering the operational constraints.

α	$RSSE$	$RSSE^*$
0	4.2764	4.2665
0.1	4.2764	4.2664
0.2	4.2766	4.2665
0.5	4.2764	4.2665
0.75	4.2763	4.2664
0.9	4.2765	4.2666
0.99	4.2764	4.2665

Table 5
RSSE for $\alpha = 0.5$ when the coding and control techniques of [17] are used.

T	$RSSE$
0.01	4.2987
0.1	8.8922
0.2	9.2540
0.5	12.2443
1	20.1553
2	180.8478

The coding techniques of [16] and [17] can be combined with other nonlinear controller techniques, such as the technique presented in [26] developed for controlling robotic manipulators subject to the bounded torque constraint in order to achieve better tele-presence and tele-operation performance. This is left for future investigation.

Conflict of Interests: None.
Financial Support: None.
Ethical Considerations: None.
Authors' Contributions: Mr. Hokmi and Mr. Haghi were Dr. Farhadi's BSc. students. They developed computer codes under Dr. Farhadi close supervision for the theoretical developments presented by Dr. Farhadi in other journal articles. Then, they performed computer simulations. Dr. Farhadi wrote and revised the paper.

References

[1] P. F. Hokayem and M. W. Spong. Bilateral teleoperation: A historical survey. *Automatica*, 42(12): 2035 - 2057, 2006.

[2] E. Nuno, I. Sarras and L. Basanez. An adaptive controller for bilateral teleoperation: Variable time-delay case. *IFAC Proceedings*, 47(3): 9341 - 9346, 2014.

[3] C. Liu, J. Guo and P. Poignet. Nonlinear model - mediated teleoperation for surgical applications under time variant communication delay. *IFAC Proceedings*, 51(22): 493 - 499, 2018.

[4] K. Yoshida and T. Namerikawa. Predictive PD control for teleoperation with communication delay. *IFAC Proceedings*, 41(2): 12703 - 12708, 2008.

[5] A. Eusebi and C. Melchiorri. Force reflecting telemanipulators with time-delay: Stability analysis and control design. *IEEE Transactions on Robotics and Automation*, 14(4): 635 - 640, 1998.

[6] T. Imaida, Y. Yokokohji, T. Doi, M. Oda and T. Yoshikwa. Groundspace bilateral teleoperation of ETS-VII robot arm by direct bilateral coupling under 7-s time delay condition. *IEEE Transactions on Robotics and Automation*, 20(3): 499 - 511, 2004.

[7] R. J. Anderson and M. W. Spong. Bilateral control of teleoperators with time delay. *Proceedings of the IEEE conference on Decision and Control*, 167 - 173, 1998.

[8] A. K. Bejczy and W. S. Kim. Predictive displays and shared compliance control for time-delayed telemanipulation. *Proceedings of the IEEE/RSJ International Conference on Intelligent Robots and Systems*, 407 - 412, 1990.

[9] A. Bemporad. Predictive control of teleoperated constrained systems with unbounded communication delays. *Proceedings of the IEEE Conference on Decision and Control*, Vol. 2: 2133 - 2138, 1998.

[10] C. Benedetti, M. Franchini and P. Fiorini. Stable tracking in variable time-delay teleoperation. *Proceedings of the IEEE/RSJ International Conference on Intelligent Robots and Systems*, Vol. 4: 2252 - 2257, 2001.

[11] P. Berestesky, N. Chopra and M. W. Spong. Discrete time passivity in bilateral teleoperation over the internet. *Proceedings of the IEEE International Conference on Robotics and Automation*, 2004.

[12] M. Dolgov, J. Fischer and U. D. Hanebeck. Event-based LQG control over networks with random transmission delays and packet losses. *IFAC Proceedings*, 46(27), pp. 23 - 30, 2013.

[13] D. Shah and A. Mehta. Discrete-time sliding mode controller subject to real-time fractional delays and packet losses for networked control system. *International Journal of Control, Automation and Systems*, 15, pp. 2690 - 2703, 2017.

[14] Yerong Sun, Yeguo Sun and C. Yang. Finite-time control of networked control systems with time delay and packet dropout. *Journal of Control Science and Engineering*, volume 2021.

[15] S. Tatikonda and S. Mitter. Control over noisy channels. *IEEE Trans. on Automatic Control*, 49(7), pp. 1196 - 1201, July 2004.

[16] A. Parsa and A. Farhadi. Measurement and control of nonlinear dynamic systems over the Internet (IoT): Applications in remote control of autonomous vehicles. *Automatica*, 95: 93 - 103, 2018.

[17] A. Parsa and A. Farhadi. New coding scheme for the state estimation and reference tracking of nonlinear dynamic systems over the packet erasure channel (IoT): Applications in tele-operation of autonomous vehicles. *European Journal of Control*, 57: 242 - 252, April 2021.

[18] A. Ustundag and E. Cevikcan. *Industry 4.0: Managing The Digital Transformation*. Springer, 2017.

[19] Vishakha and S. Jain. Big data analytics as a solution for threat analysis and risk mitigation in smart cities: A review. *International Research Based Journal*, 6(1), 2017.

[20] J. J. Slotine and W. Li. *Applied Nonlinear Control*. Prentice-Hall, 1991.

[21] K. Ogata. *Discrete - Time Control Systems*. Prentice Hall, 1987.

[22] C. Chen, C. Zhang, T. Hu, H. Ni and Q. Chen. Finite-time tracking control for uncertain robotic manipulators using backstepping method and novel extended state observer. *International Journal of Advanced Robotic Systems*, May - June 2019.

[23] D. E. Kirk. *Introduction to Optimal Control Theory: An Introduction*. Dover Publications; Illustrated edition (26 April 2012).

[24] H. Lin and P. J. Antsaklis. Stability and stabilizability of switched linear systems: A survey of recent results. *IEEE Transactions on Automatic Control*, 54(2), 308 - 322, 2009.

[25] G. Zhai, B. Hu, K. Yasuda and A. N. Michel. Qualitative analysis of discrete-time switched systems. *in Proceedings of the American Control Conference*, 1880 - 1885, 2002.

[26] W.E. Dixon, M.S. de Queiroz, F. Zhang and D.M. Dawson. Tracking control of robot manipulators with bounded torque inputs. *Robotica*, vol. 17, 121 - 129, 1999.